STRANGE PARTICLE PRODUCTION IN SULPHUR-TUNGSTEN INTERACTIONS AT 200 GEV/C PER NUCLEON

Presented by: J.B. Kinson, University of Birmingham

The WA85 Collaboration

S. Abatzis[1], F. Antinori[5], R.P. Barnes[4], A.C. Bayes[4], M. Benayoun[6], W. Beusch[5], I.J. Bloodworth[4], A. Bravar[7], J.N. Carney[4], B. de la Cruz[5a], D. Di Bari[2], J.P. Dufey[5], D. Evans[4], R. Fini[2], B.R. French[5], B. Ghidini[2], M. Girone[2], H. Helstrup[3], A.K. Holme[3], A. Jacholkowski[5], J. Kahane[6], J.B. Kinson[4], A. Kirk[5], K. Knudson[5], J.C. Lassalle[5], V. Lenti[2] , Ph. Leruste[6], L. Lima Francês[6], R.A. Loconsole[2], A. Malamant[6], V. Manzari[2], F. Navach[2], J.L. Narjoux[6], A. Palano[2], A. Penzo[7], E. Quercigh[5], L. Rossi[5b], K. Šafařik[6], M. Sené[6], R. Sené[6], M. Tamazouzt[6], M.T. Trainor[5c], G. Vassiliadis[1], O. Villalobos Baillie[4], A. Volte[5] and M.F. Votruba[4]

1. Athens University, Athens, Greece
2. Università di Bari and Sezione INFN, Bari, Italy
3. Universitetet i Bergen, Bergen, Norway
4. University of Birmingham, Birmingham, U.K.
5. CERN, European Organization for Nuclear Research, Geneva, Switzerland
6. Collège de France, Paris, France
7. INFN, Trieste, Italy

[a]On leave from CIEMAT, Madrid, Spain

[b]Now at INFN, Genoa, Italy

[c]Now at Oxford University, Oxford, U.K.

Abstract

Multi-strange baryon and anti-baryon production is expected to be a useful probe in the search for Quark-Gluon Plasma formation. We present the transverse mass distributions of negative particles, K^0s, Λs, $\bar{\Lambda}$s, and Ξ^-s produced in sulphur-tungsten interactions at 200 GeV/c per nucleon and give the corrected ratios $\bar{\Lambda}/\Lambda$, Ξ^-/Λ and $\bar{\Xi}^-/\bar{\Lambda}$. We note that our ratio $\bar{\Xi}^-/\bar{\Lambda}$ appears large in comparison to that from p p interactions.

Presented at Quark Matter '91, Gatlinburg, Tennessee, USA, November 1991

1. INTRODUCTION

Hyperon production is expected to be a useful probe of the dynamics of hadronic matter under the extreme conditions realised in central heavy ion collisions [1]. In particular, the onset of a Quark-Gluon Plasma (QGP) phase during the collisions is expected to enhance the antihyperon yield with respect to normal hadronic interactions and to give rise to a large $\bar{\Xi}^-/\bar{\Lambda}$ ratio [2]. WA85 is the only experiment which has obtained results on the production of cascades in heavy ion interactions. In this paper we present the transverse mass distributions for negative particles (mostly pions), K^os, Λs, $\bar{\Lambda}$s and Ξ^-s produced in S-W interactions at 200 GeV/c per nucleon. We give the $\bar{\Lambda}/\Lambda$, Ξ^-/Λ and $\bar{\Xi}^-/\bar{\Lambda}$ ratios, where the Λs ($\bar{\Lambda}$s) are corrected for contamination from Ξ ($\bar{\Xi}$) decays.

The WA85 experiment [3] was performed using the CERN Omega Spectrometer with a 200 GeV/c per nucleon beam of ^{32}S ions incident on a tungsten target. The aim is to study strangeness production at $p_T > 1$ GeV/c and central rapidity. The Omega multiwire proportional chambers were modified to select only high p_T tracks so that only a few tracks are recorded out of the several hundred produced in a central collision making reconstruction of both strange and multi-strange baryons possible in this kinematic region.

2. APPARATUS AND TRIGGER

The main problem in the experimental study of heavy ion collisions is posed by the very high event multiplicities. There are several different strategies for coping with these conditions. The WA85 experiment measures tracks in a restricted kinematic range ($2.3 < y_{lab} < 3$, $p_T > 0.6$ GeV/c). This (i) simplifies the reconstruction of tracks, allowing the identification of complicated topologies with good reconstruction efficiencies, and (ii) allows the event records to be kept small, resulting in a rapid event collection rate.

The layout of the experiment [3] is shown in Fig. 1. An upstream quartz Cerenkov counter identifies incoming sulphur ions, which are incident on a thin tungsten target (0.5% interaction length). An array of microstrip counters placed close to the target (see inset) samples the charged particle multiplicity at central rapidities, i.e. in the pseudorapidity range $2.1 < \eta < 3.4$. The total number of strips hit in the upper and lower microstrip arrays (microstrip multiplicity) is found by simulation to be proportional to the overall charged multiplicity at central rapidities. Particle tracking is performed in 21 planes of Multi Wire Proportional Chambers (MWPC) placed between 2.3 and 4.1 metres from the target. The sensitive region of the chambers has a "butterfly" geometry [4]. Only tracks with $p_T > 0.6$ GeV/c can reach this region from the target through the magnetic field. The track multiplicity recorded in the Omega MWPCs, is about 1% of the overall

charged multiplicity. Two hodoscopes (HZ0 and HZ1) with a butterfly geometry matching that of the chambers are placed downstream for triggering purposes. Finally, a veto hadron calorimeter placed 25 metres downstream of the target is used to reject events with large forward energy.

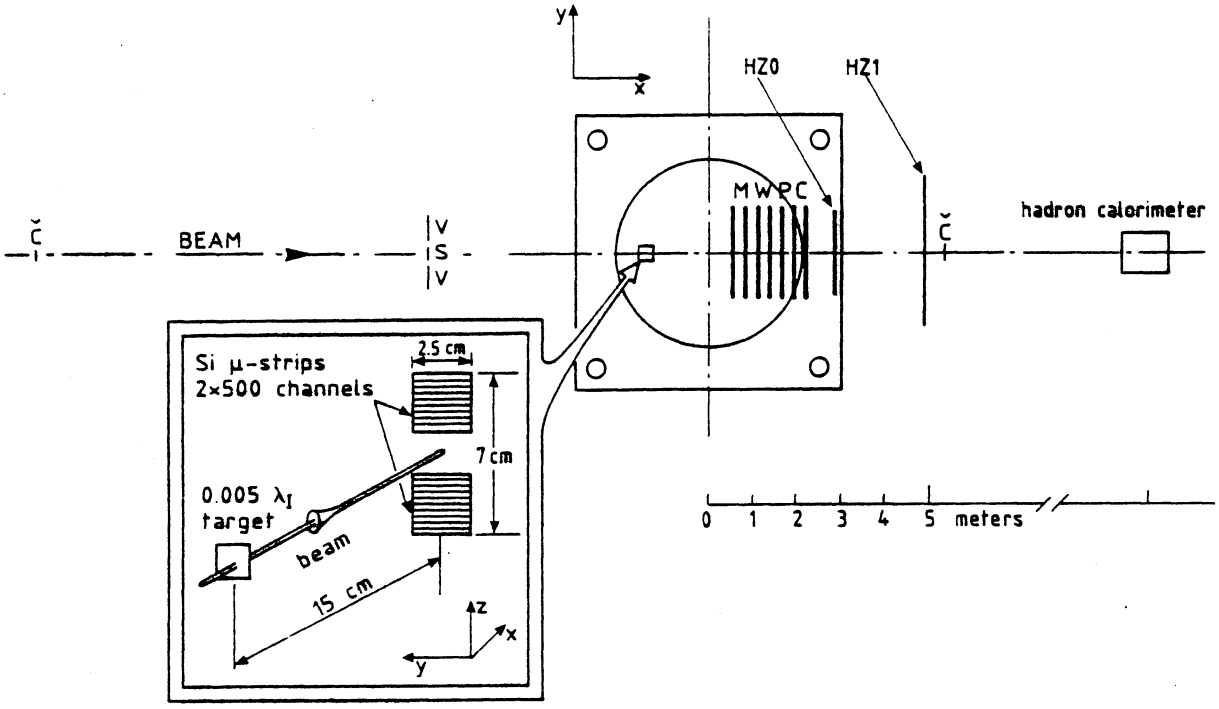

Figure 1. Layout of the WA85 experiment.

3. SELECTION OF STRANGE PARTICLE DECAYS

The procedure used for selecting V° and cascade candidates has been described in detail elsewhere[5]. A pair of oppositely charged tracks is considered a V° candidate if the tracks intersect at a point well separated from the target (at least 1.4 metres), which is taken as the V° vertex (Fig. 2). The V° momentum vector should point along the direction of the line of flight from the V° vertex to the target. The V° decay tracks should miss the target when projected back through the magnetic field to the target plane.

Mass distributions for V° candidates are shown in Fig. 3 for the 1987 S-W data. We select candidates in a 50 MeV mass interval centred on the Λ mass, giving 13307 Λ and 3407 $\bar{\Lambda}$ candidates. In the case of the K^0 a mass interval of 100 MeV is used, giving 2753 candidates.

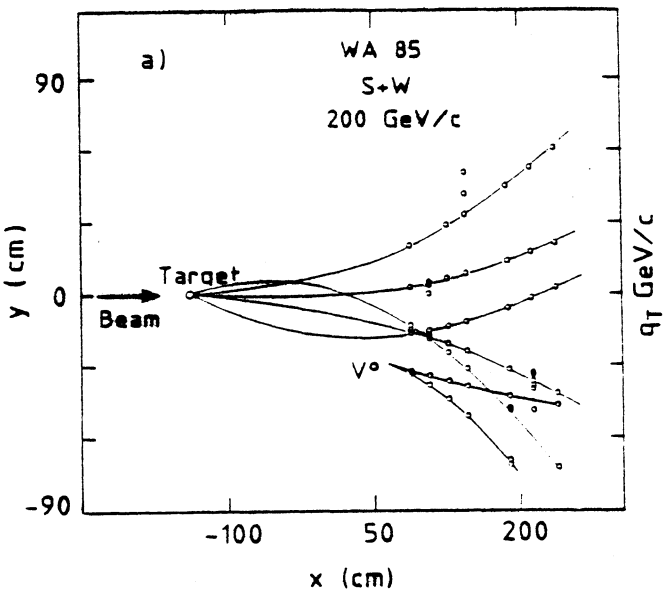

Figure 2. Reconstructed event with a V^0.

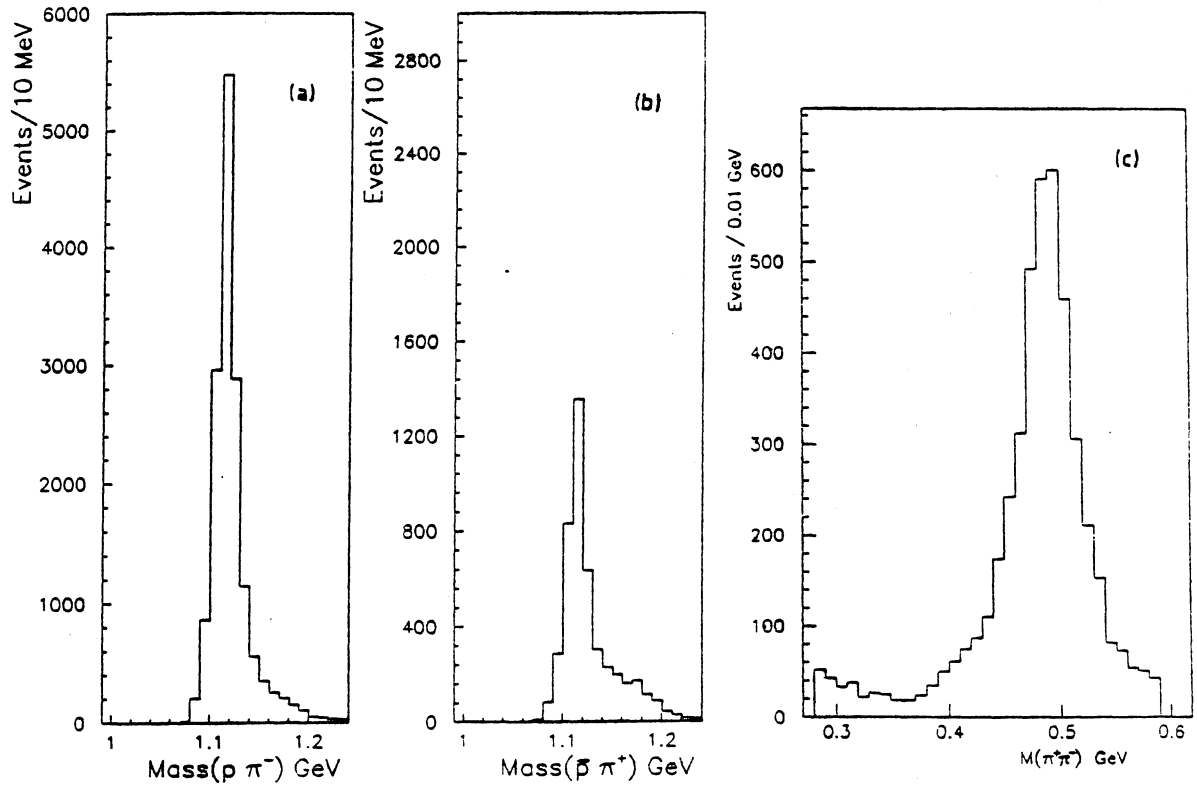

Figure 3. Mass distributions for V^0 candidates as (a) $p\pi^-$, (b) $\bar{p}\pi^+$ and (c) $\pi^+\pi^-$.

The method of selecting Ξ^- ($\bar{\Xi}^+$) decays has also been described previously [6]. In this case the Λ ($\bar{\Lambda}$) is not required to point back to the target. A charged track, which does not come from the target, is required to intersect the line-of-flight of the Λ ($\bar{\Lambda}$). The resulting Ξ^- ($\bar{\Xi}^+$) momentum vector should point back to the target and the cascade decay should take place at least 100 cm from the target. Fig. 4 shows a fully reconstructed event with an $\bar{\Xi}^+$ candidate.

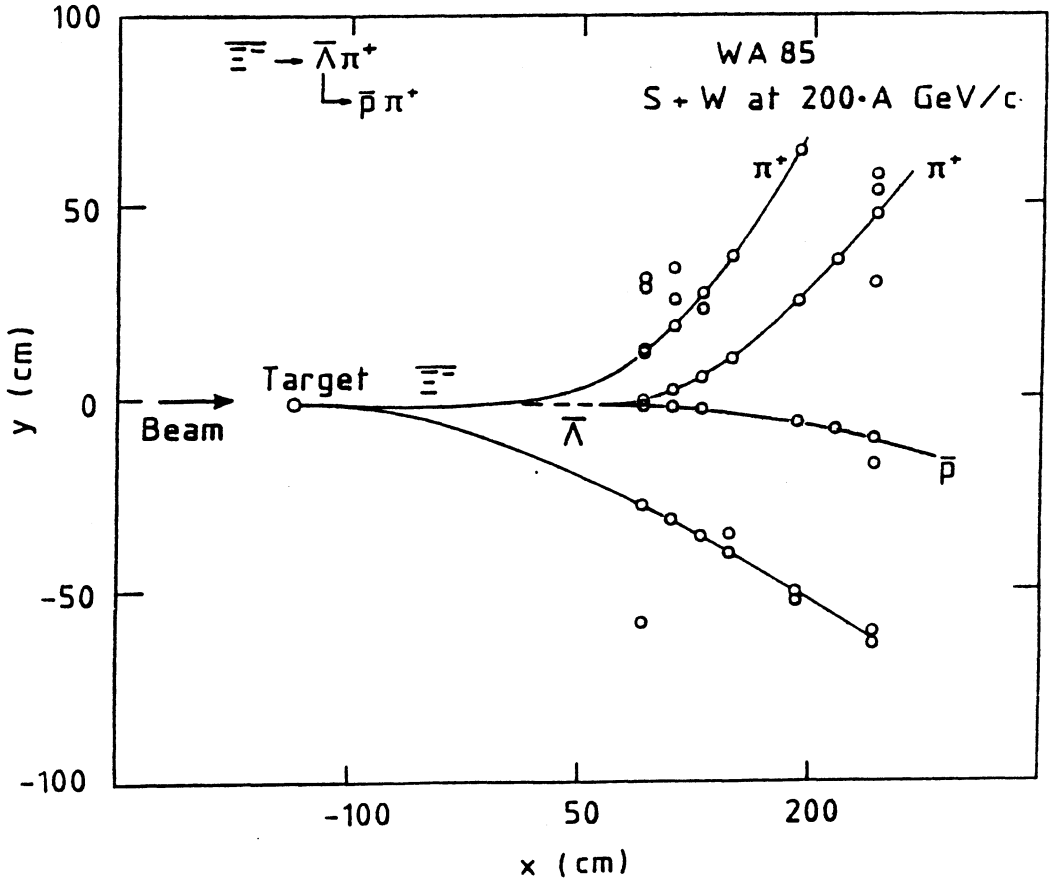

Figure 4. Reconstructed event with a cascade candidate.

Mass distributions for cascade candidates are shown in Fig. 5. Clear peaks are seen at the Ξ^- and $\bar{\Xi}^+$ positions with little background. Selecting events in a 100 MeV mass interval centred on the Ξ^- mass gives 108 Ξ^- and 44 $\bar{\Xi}^+$ candidates.

The full phase space window used for Λs and $\bar{\Lambda}$s is $2.3 < y_{lab} < 3.0$ and $0.9 < p_T < 2.8$ GeV/c; for Ξ^-s and $\bar{\Xi}^+$s it is $2.3 < y_{lab} < 3.0$ and $1.1 < p_T < 3.3$ GeV/c.

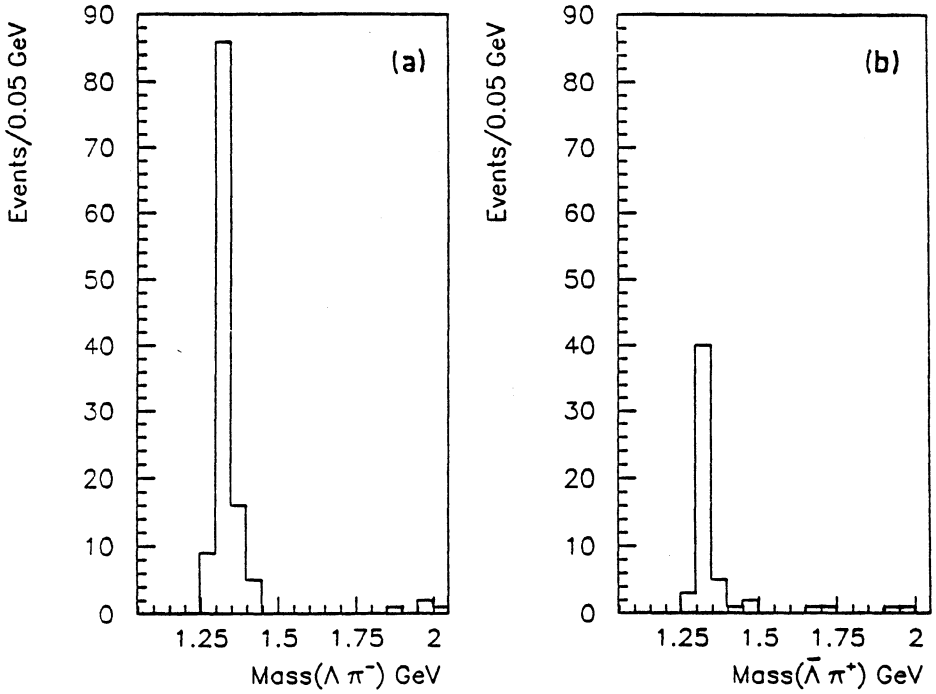

Figure 5. Mass distributions for cascade candidates as (a) $\Lambda\pi^-$ and (b) $\bar{\Lambda}\pi^+$.

4. DATA SAMPLES

The results in this paper are based on 10 million S-W events obtained in 1987 and 18 million p-W events obtained in 1988. The V^0 and Ξ yields from these data are shown in Table 1. In 1990 80 million S-W events and 100 million p-W events were recorded and analysis is still in progress. Preliminary mass distributions for Λ candidates are shown in Fig. 6. Selecting candidates in 50 MeV mass intervals centred on the Λ mass gives 67000 Λs from half of the S-W data and 26000 Λs from half of the p-W data. A further 100 million S-S events have been obtained recently.

Table 1
Yields for different particle species; 1987 and 1988 data

Species	S-W	p-W
Λ	13307	3223
$\bar{\Lambda}$	3407	959
K^0_S	2753	1001
Ξ^-	108	82
$\bar{\Xi}^+$	44	22

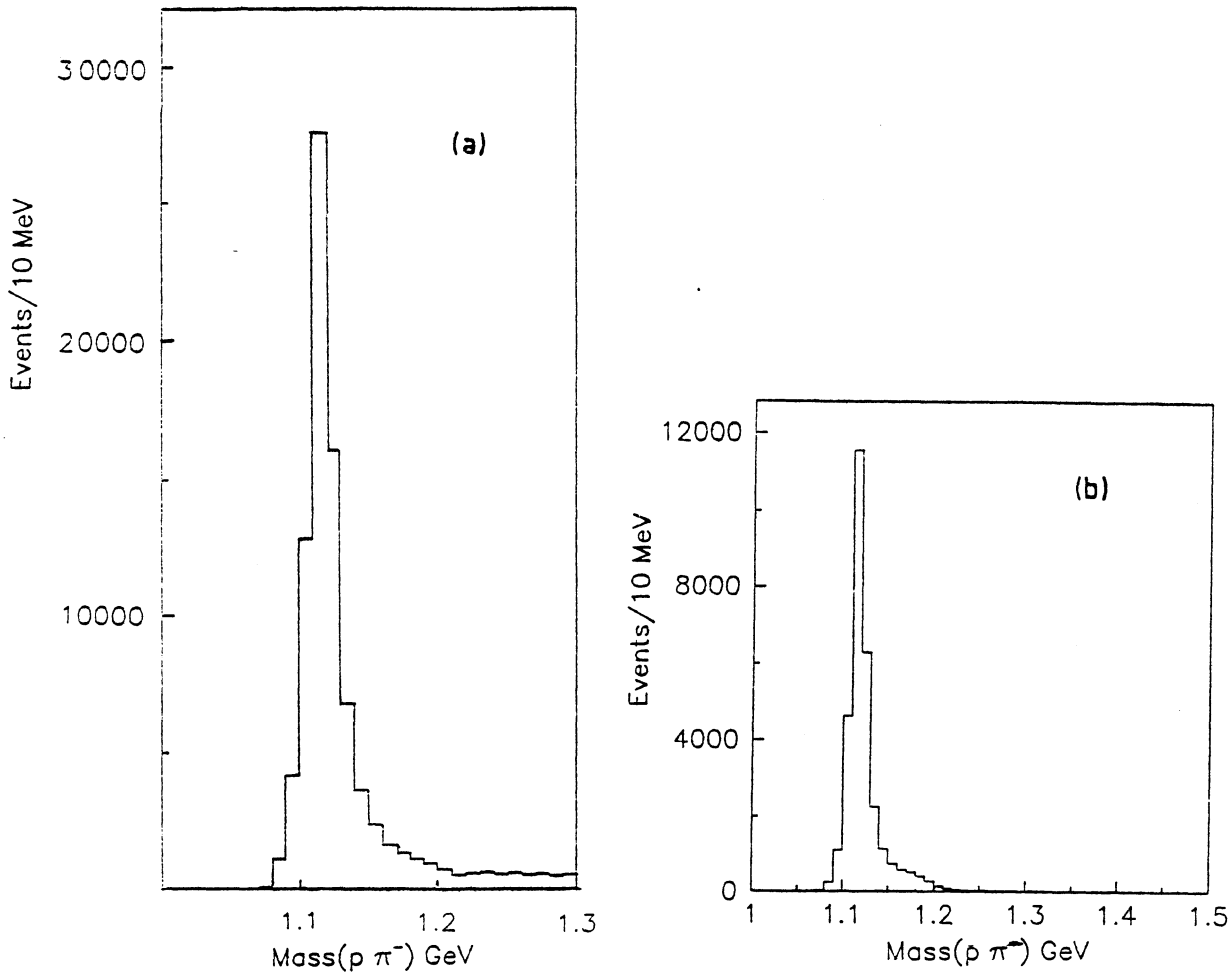

Figure 6. Preliminary mass distributions for V^0 candidates from the 1990 data, (a) S-W and (b) p-W.

5. RESULTS

5.1. Multiplicity dependences

A study of Λ, $\bar{\Lambda}$ and negative hadron production as a function of the charged multiplicity measured by the silicon microstrips has been published [5]. Negative hadrons detected in the butterfly MWPCs are considered in the same rapidity and p_T region as that defined for the Λ and $\bar{\Lambda}$ samples. Fig. 7a shows the average number of negative hadrons per event, $<n_->$, as a function of multiplicity, corrected for geometrical acceptance (triangles) and for both geometrical acceptance and track reconstruction efficiency (circles). A simulation study [5] shows that the mean rapidity density for tracks in the region $2.3 < y_{lab} < 3.0$ is proportional to the microstrip multiplicity and it is shown in the lower scales of Fig. 7.

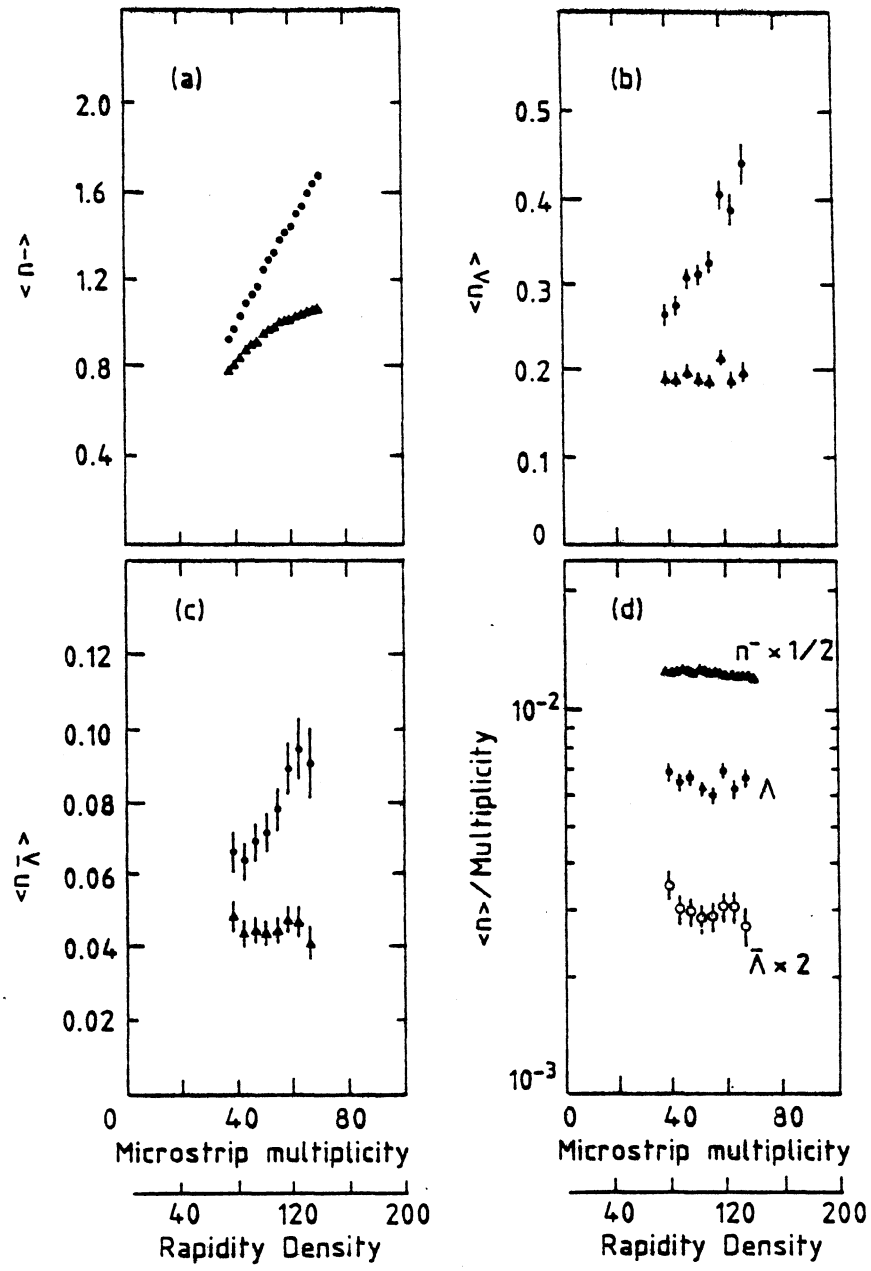

Figure 7. (a) $<n->$, (b) $<n_\Lambda>$ and (c) $<n_{\bar{\Lambda}}>$ as a function of measured multiplicity: circles show data corrected for geometrical acceptance and reconstruction efficiency and triangles show data with acceptance correction only. The errors are statistical only. (d) $<n->$/multiplicity, $<n_\Lambda>$/multiplicity and $<n_{\bar{\Lambda}}>$/multiplicity as a function of multiplicity. Points for negative particles have been divided by 2, points for $\bar{\Lambda}$ have been multiplied by 2. The data are corrected for geometrical acceptance and reconstruction efficiency. The lower scale shows the average rapidity densities (evaluated in the interval $2.3 < Y_{lab} < 3.0$) which correspond to the measured multiplicity.

Figs. 7b and 7c show the average number of Λ and $\bar{\Lambda}$ per event, $<n_{\Lambda}>$ and $<n_{\bar{\Lambda}}>$ respectively, as a function of multiplicity. The data are corrected for geometrical acceptance, including correction for decays outside the fiducial region and unseen decay modes (triangles) and in addition reconstruction efficiency (circles). The reconstruction efficiencies have been determined by implanting simulated Λ, $\bar{\Lambda}$ and π^- in real events of varying multiplicity. They vary from 90% to 60% for single tracks and from 85% to 40% for Λ and $\bar{\Lambda}$ as the multiplicity increases. The ratios of Λ, $\bar{\Lambda}$ and negative hadron yields to multiplicity are shown in Fig. 7d as a function of multiplicity. They are essentially constant over the multiplicity range considered.

Similar plots for K^os are shown in Fig. 8. The average number of K^os also shows a linear rise over the multiplicity range investigated. Thus we find no evidence for a faster than linear increase for negative hadrons, Λ, $\bar{\Lambda}$ and K^os over the rapidity density range $70 < dN/dy < 140$.

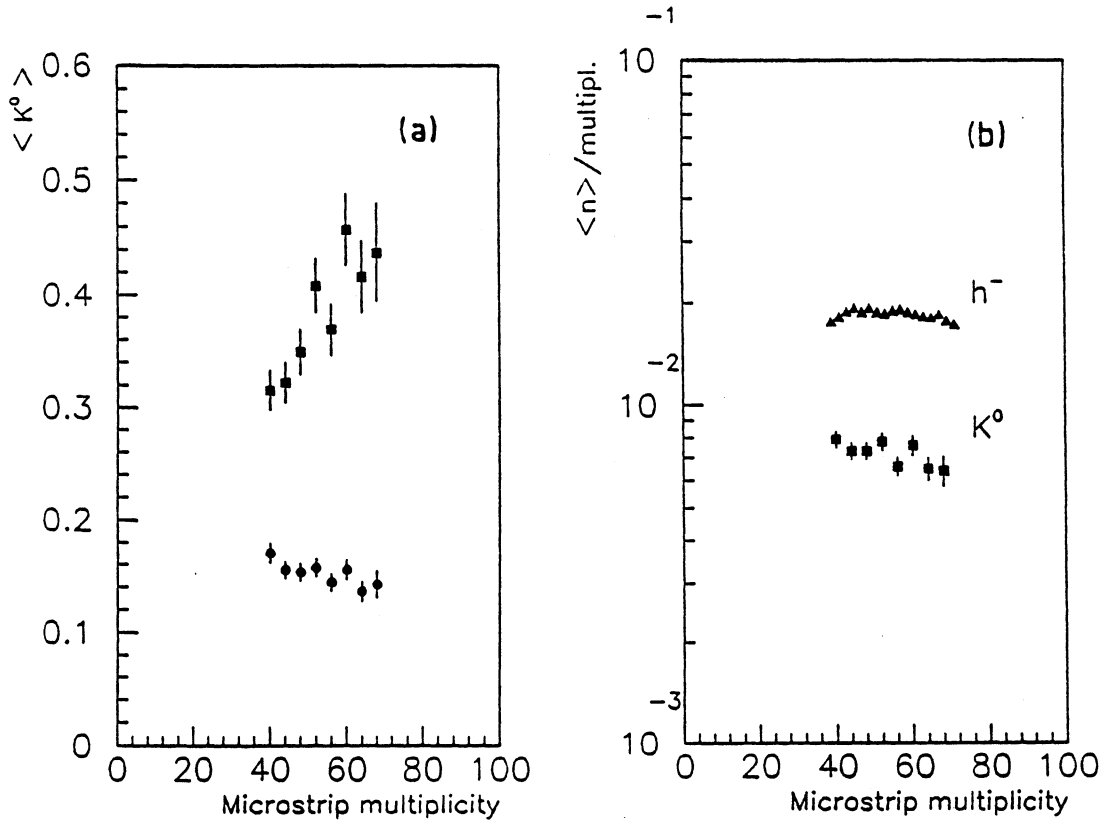

Figure 8. (a) $<n_{K^o}>$ as a function of measured multiplicity. (b) $<n->$/multiplicity and $<n_{K^o}>$/multiplicity as a function of multiplicity.

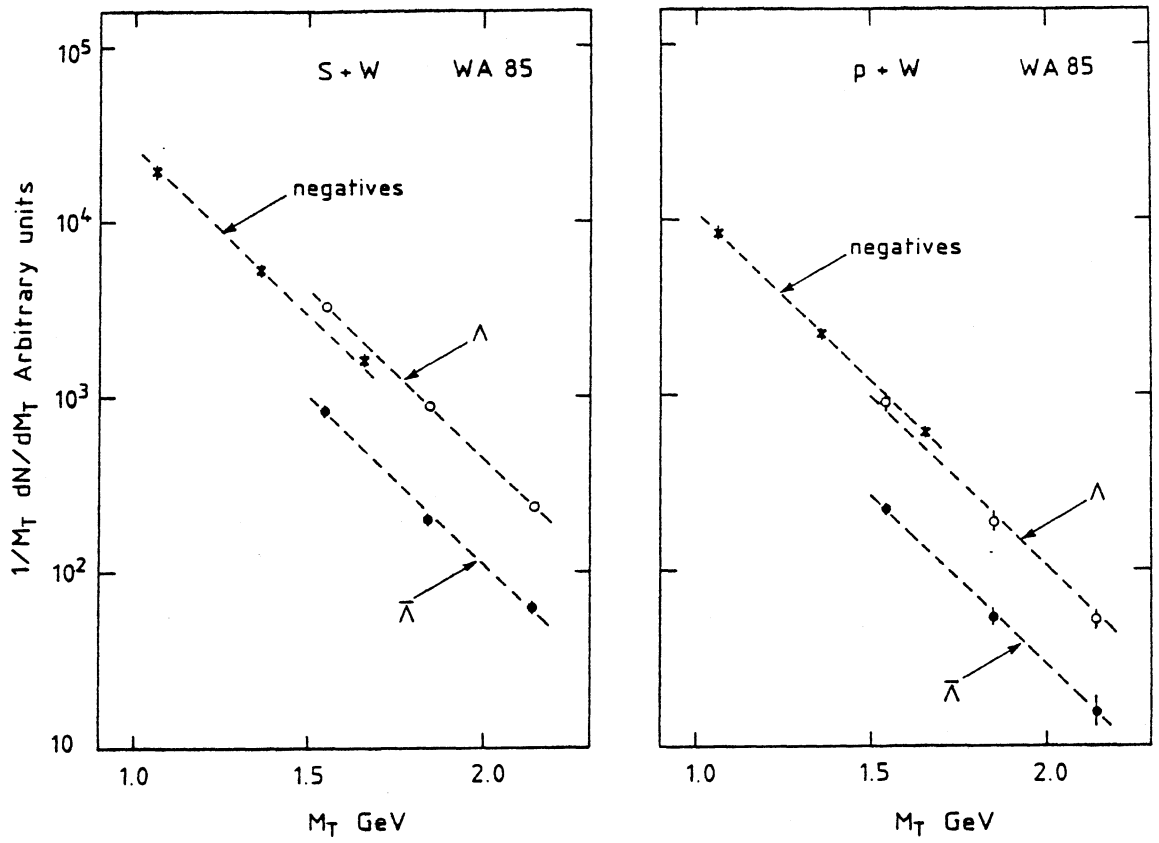

Figure 9. Transverse mass distributions for Λ, $\bar{\Lambda}$ and h^- in S-W and p-W interactions.

5.2. Transverse mass distributions

The invariant transverse mass distributions $(1/m_T)\ dN/dm_T$ have been studied for Λ, $\bar{\Lambda}$, K^0 and h^- in both p-W and S-W collisions [7,8]: the distributions are shown in Figs. 9 and 10. The slopes for all the distributions are similar, and for all the species considered indicate an increase by a factor of about 2 in the ratio of strange particle to negative production in S-W relative to p-W interactions.

The invariant transverse mass distributions fall exponentially with increasing m_T [8,9] according to

$$\frac{1}{m_T}\frac{dN}{dm_T} = \exp\left[-\frac{m_T}{\tau}\right]$$

The inverse slopes τ of these distributions provide valuable information as to the temperature of the fireball from which they are produced. Fig. 11 shows the

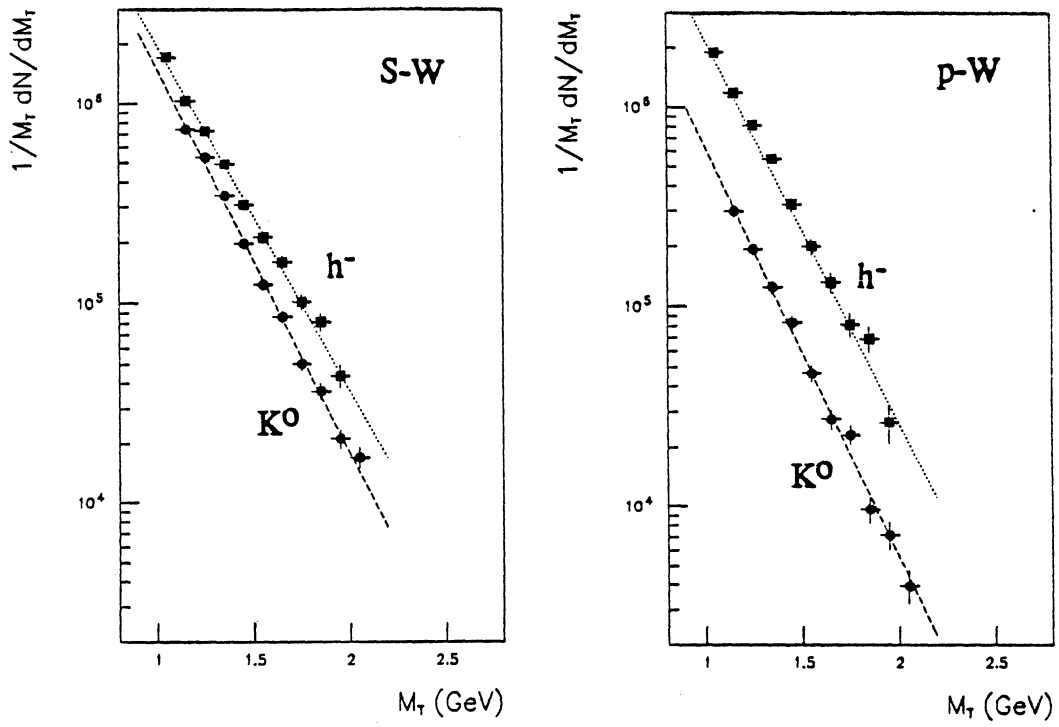

Figure 10. Transverse mass distributions for K^0s and h^- in S-W and p-W.

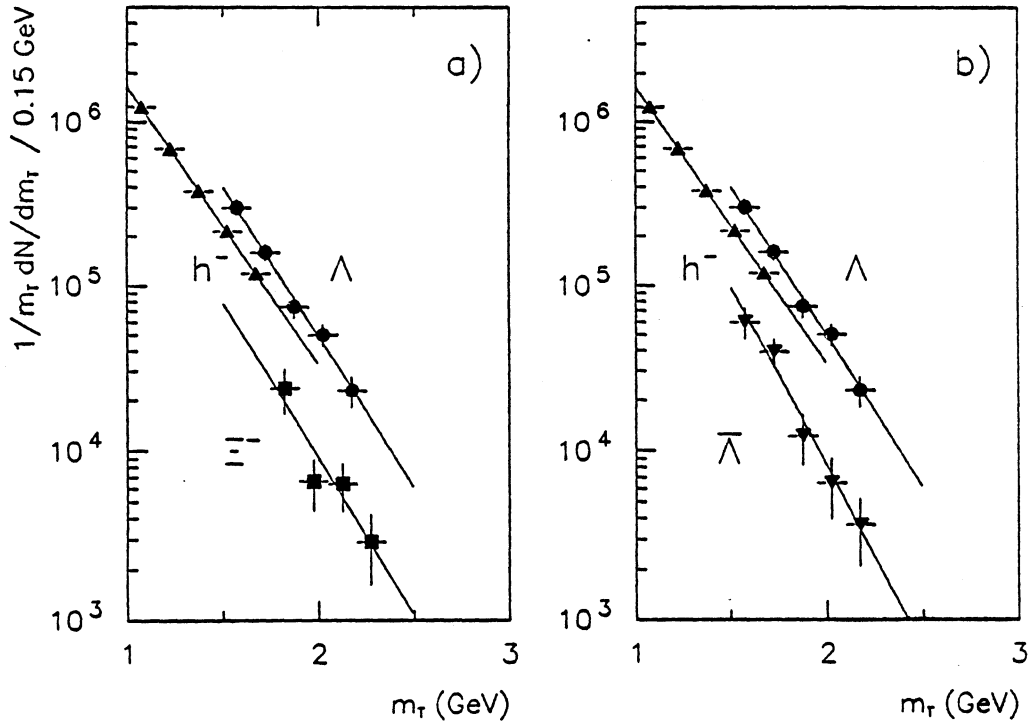

Figure 11. Transverse mass distributions in S-W interactions for (a) Λ, h^- and Ξ^- and (b) Λ, h^- and $\bar{\Lambda}$.

invariant m_T distribution in S-W interactions for Λ, $\bar{\Lambda}$, Ξ^- and h^-. Here in addition to corrections for acceptance and reconstruction efficiency, the Λ and $\bar{\Lambda}$ distributions have also been corrected for feed-down from Ξ and $\bar{\Xi}$ decay [10]. The inverse slopes obtained from the distributions in Fig. 11, and from Fig. 10 for K^o, are given in Table 2. The inverse slopes for all the species considered are compatible with a value of about 230 MeV.

Table 2.
Inverse slopes of m_T distributions for different particle species (MeV).

Species	S-W	p-W
h^-	$256 \pm 3 \pm 15$	$226 \pm 4 \pm 15$
Λ	$238 \pm 9 \pm 15$	–
$\bar{\Lambda}$	$201 \pm 24 \pm 15$	–
K^o_S	$224 \pm 5 \pm 15$	$211 \pm 5 \pm 15$
Ξ^-	$233 \pm 54 \pm 15$	–

5.3. Strange and multistrange baryon and antibaryon ratios

Once corrections have been made to particle production rates to allow for acceptance, reconstruction efficiency, particle identification and feed-down, it is possible to compare production rates for the hyperons and antihyperons [10]. The hyperon-antihyperon ratios $\bar{\Lambda}/\Lambda$ and $\bar{\Xi}^-/\Xi^-$ are straightforward to calculate; however, the values obtained for the Ξ^-/Λ and $\bar{\Xi}^-/\bar{\Lambda}$ ratios depend on whether a cut is made in p_T or m_T, owing to the different rest masses for the Ξ and the Λ. In Table 3 we present the ratios (i) in terms of an m_T cut, and (ii) in the p_T range $1 < p_T < 2$ GeV/c in order to facilitate comparison with other experiments. In addition,

Table 3
Relative hyperon production rates for S-W data

Ratio	$m_T > 1.72$ GeV	$1 < p_T < 2$ GeV/c
$\bar{\Lambda}/\Lambda$	0.13 ± 0.03	0.13 ± 0.03
$\bar{\Xi}^-/\Xi^-$	0.39 ± 0.07	0.39 ± 0.07
Ξ^-/Λ	0.20 ± 0.04	0.11 ± 0.02
$\bar{\Xi}^-/\bar{\Lambda}$	0.6 ± 0.2	0.33 ± 0.11

a preliminary study of cascade production in p-W interactions gives the values $\bar{\Xi}^- / \Xi^- = 0.27 \pm 0.06$ [11], not corrected for acceptance or reconstruction efficiency. The $\overline{\Xi^-} / \Xi^-$ ratio appears to be higher in S-W than in p-W interactions, while the $\bar{\Xi} / \bar{\Lambda}$ ratio appears high in comparison with all other published values (from e^+e^-, $\bar{p}p$ and pp interactions [12]) as shown in Fig. 12.

All these values point towards a considerable degree of flavour equilibration in central nucleus interactions at a temperature (from the inverse slope of the m_T distribution) close to that at which a phase transition is expected to occur. The errors are at present dominated by statistics, but will be reduced substantially when the 1990 data are analysed.

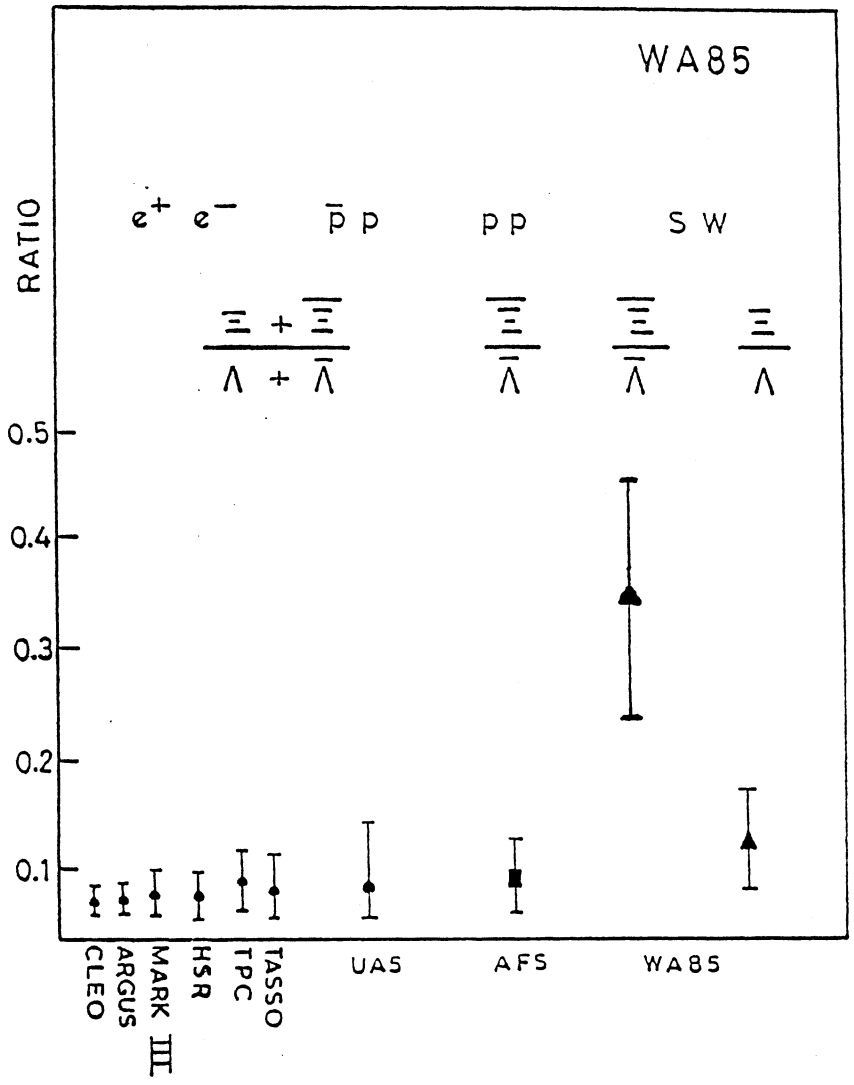

Figure 12. Ξ^-/Λ and $\bar{\Xi}^-/\bar{\Lambda}$ ratios for different experiments.

6. CONCLUSIONS

The WA85 experiment has studied strange particle production in S-W and p-W interactions at 200 GeV/c per nucleon. A general strangeness increase by a factor of about 2 has been observed in S-W interactions relative to p-W interactions. The average number of negative particles, K^0s, Λs and $\bar{\Lambda}$s shows a linear rise over the rapidity density range $70 < dN/dy < 140$.

The transverse mass distributions for K^0, Λ, $\bar{\Lambda}$, and Ξ^- have inverse slopes compatible with a value of about 230 MeV. The $\bar{\Xi}^-/\Xi^-$ ratio in S-W interactions is 0.39 ± 0.06, which appears to be higher than in p-W interactions. The $\bar{\Xi}^-$ / $\bar{\Lambda}$ ratio in S-W interactions is found to be 0.6 ± 0.2 for $m_T > 1.72$ GeV. These ratios are high compared with what is expected from current non-QGP models and suggest that some flavour equilibration has taken place.

REFERENCES

1. J. Rafelski, Phys. Rep. **88** (1982) 331.
   J. Rafelski and B. Muller, Phys. Rev. Lett. **48** (1982) 1066.
   P. Koch, B. Muller and J. Rafelski, Phys. Rep. **142** (1986) 167.
   J. Ellis and U. Heinz, Phys. Lett. **233B** (1989) 223.
2. J. Rafelski, AZPH-TH/91-11 (1991), submitted to Phys. Lett. B.
3. WA85 Proposal, CERN/SPSC 84-76 P206 (1984).
   CERN/SPSC 87-18 P206 Add. (1987).
   CERN/SPSC 88-20 P206 Add. (1988).
4. W. Beusch et al., Nucl. Inst. and Methods, **A249** (1986) 391.
5. S. Abatzis et al., Phys. Lett. **244B** (1990) 130.
6. S. Abatzis et al., Phys. Lett. **259B** (1991) 508.
7. S. Abatzis et al., Nucl. Phys. **A525** (1991) 445c.
8. S. Abatzis et al., Proc. Int. Europhysics Conf. on High Energy Physics, Geneva 1991. Presented by B. Ghidini.
9. B. Jacak, Nucl. Phys. **A525** (1991) 77c.
10. S. Abatzis et al., Phys. Lett. **270B** (1991) 123.
11. S. Abatzis et al., Nucl. Phys. **A525** (1991) 441c.
12. AFS Coll., T. Akesson et al., Nucl. Phys. **B246** (1984) 1.
    UA5 Coll., R.E. Ansorge et al., CERN-EP/89-41.
    TASSO Coll., M. Althoff et al., Phys. Lett. **130B** (1983) 340.
    MARK II Coll., S.R. Klein et al., Phys. Rev. Lett. **58** (1987) 644.
    TPC Coll., H. Yamamoto, Proc XX Rencontres de Moriond (1986).
    CLEO Coll., M.S. Alam et al., Phys. Rev. Lett. **53** (1984) 24.
    ARGUS Coll., A. Albrecht et al., Phys. Lett. **183B** (1987) 419.
    HRS Coll., S. Abachi et al., Phys. Rev. Lett. **58** (1987) 2627.